

# Design of Navigation Environment Generation Module of M&S Software for Integrated Navigation System Performance Evaluation

Heyone Kim<sup>1</sup>, Junhak Lee<sup>1</sup>, Sang Heon Oh<sup>2</sup>, Hyounghmin So<sup>3</sup>, Dong-Hwan Hwang<sup>1†</sup>

<sup>1</sup>Department of Electronics Engineering, Chungnam National University, Daejeon 34140, Korea

<sup>2</sup>Navcours Co. Ltd, Daejeon, Korea

<sup>3</sup>Agency for Defense Development, Korea

## ABSTRACT

Various navigation systems are integrated with the Global Navigation Satellite System (GNSS) to improve navigation performance so that continuous navigation information can be obtained even when navigation performance is degraded or navigation is not available due to the outage of GNSS. Time and cost can be reduced by evaluating performance of the integrated navigation system through Modeling and Simulation (M&S) software prior to the deployment of the integrated navigation system. The measurements of the navigation system should be generated to evaluate performance through of the navigation system M&S software. This paper proposes a method of designing a navigation environment generation module in M&S software of the integrated navigation system. To show applicability of the proposed method to M&S software design of the integrated navigation system, functions are verified through MATLAB. And then visual C++ based M&S software for the integrated navigation system is implemented to check the operation of the navigation environment generation module. The reference trajectory is generated and true measurements of Global Positioning System (GPS), Korea Positioning System (KPS), and enhanced Long range navigation (eLoran) are generated from the reference trajectory. The navigation results obtained from the true measurements are compared with the reference trajectories. The results show that the measurements generated using the design generation module by the proposed method are valid and the navigation environment generation module can be applied to M&S software of the integrated navigation system.

**Keywords:** radio navigation, integrated navigation system, navigation environment generation, modeling and simulation software

## 1. INTRODUCTION

A reliable and continuous navigation results can be obtained if a number of radio navigation systems are used when navigations through GNSS are not available or navigation performance is degraded due to intentional radio interference such as jamming or spoofing (White et al. 1998, Kaplan & Hegarty 2006). One of the research results on integration of the GNSS with other terrestrial radio navigation systems is the Alternative Positioning, Navigation and

Timing (APNT) plan by the Federal Aviation Administration (Department of Transportation 2007, Department of Defense 2010). In the APNT plan, integrated system is proposed using Distance Measuring Equipment (DME) that can maintain navigation performance even when navigation through GPS are not available or navigation performance is degraded (Williams et al. 2008, Eldredge et al. 2010, Lo et al. 2010). The UK proposed an alternative navigation system which integrates the eLoran in order to reduce dependency on GPS in marine environments (Williams et al. 2008).

Before the integrated navigation systems are deployed, various functions in the system are checked and navigation performance of the system is evaluated. M&S software can be used to reduce time and cost consumed in this process (Maria 1997, Lee 2007).

---

Received Feb 19, 2018 Revised Mar 20, 2018 Accepted Apr 23, 2018

†Corresponding Author

E-mail: dhhwang@cnu.ac.kr

Tel: +82-42-821-5670 Fax: +82-42-823-5436

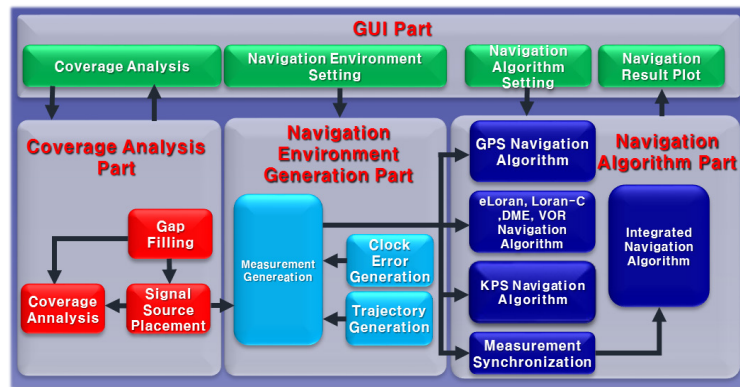


Fig. 1. Integrated navigation M&S software structure.

When performance of radio navigation systems is evaluated through M&S software, environments where radio navigation receivers are operated can be simulated using a software-based signal generator. In relation to this, research results on software-based signal generators can be found. To evaluate performance of GPS Software Defined Radio (SDR) receiver, the University of Calgary designed a software-based Intermediate Frequency (IF) GPS signal generator for L1 Coarse/Acquisition code (Dong et al. 2004). Chungnam National University also designed a software-based GPS spoofing signal generator to evaluate an anti-spoofing algorithm for GPS receivers (Lim et al. 2008). In addition, the Korea Electronics and Telecommunications Research Institute designed a GNSS signal generation simulator consisting of satellite orbit generation unit, navigation message generation unit, error generation unit, and IF signal generation unit to develop and verify the satellite navigation algorithm (Kim et al. 2009). Chungnam National University designed a GNSS multi-band IF signal generation software that can generate GPS L1/L2/L5 signals and Galileo E1/E5 signals, and verified its performance using a commercial software based GPS L1 receiver (Cho et al. 2012). In addition, Chungnam National University designed a GPS/Inertial Measurement Unit (IMU) data generator that generates GPS signals and IMU data in an M&S software that evaluates the performance of the ultra-tightly coupled GPS/INS (Ji et al. 2012).

Although research results on GPS signal generators or data generator software have been introduced, it is necessary to have a software-based navigation environment generation module that can generate measurements of various radio navigation systems including GNSS as well as terrestrial radio navigation systems to evaluate performance of the integrated navigation system. Research results on the previously mentioned GPS signal generators aim to evaluate the performance of GNSS SDR receivers or ultra-tightly coupled GPS/INS integrated navigation system.

This paper proposes a design method of navigation environment generation module of M&S software for performance evaluation of the integrated navigation system of GNSS and terrestrial radio navigation systems. A navigation environment generation module that generated measurements of GPS, KPS, and eLoran is designed. Performance is verified first through MATLAB. To show that the proposed navigation environment generation module can be used in the M&S software for performance evaluation of the integrated navigation system, an M&S software is implemented.

In Section 2, M&S software for performance evaluation of the integrated navigation system is briefly explained. In Section 3, the design method of the navigation environment generation module that generates measurements of the navigation algorithm is described. In Section 4, results of validity of the navigation environment generation module through MATLAB are presented and applicability of this to the M&S software is demonstrated. Finally, in Section 5, concluding remarks and further studies are presented.

## 2. M&S SOFTWARE OF INTEGRATED NAVIGATION SYSTEM

The M&S software of the integrated navigation system provides the navigation environments and performance evaluation results according to the design specifications of the integrated navigation system. It also shows an area where a given required navigation performance is satisfied and provides a function that derives a position of additional signal source to maximize the area if the area is not suitable for the operation of the navigation system. A navigation algorithm and measurements which are inputs of the algorithm are needed to evaluate performance. Furthermore, the integrated navigation system can be developed more effectively if

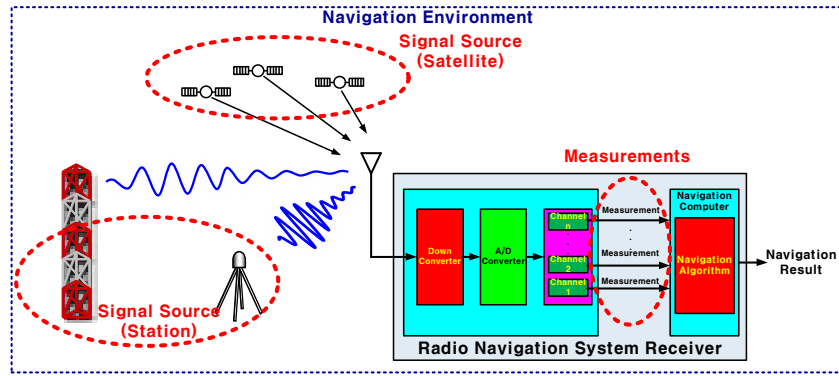


Fig. 2. Navigation environment generation.

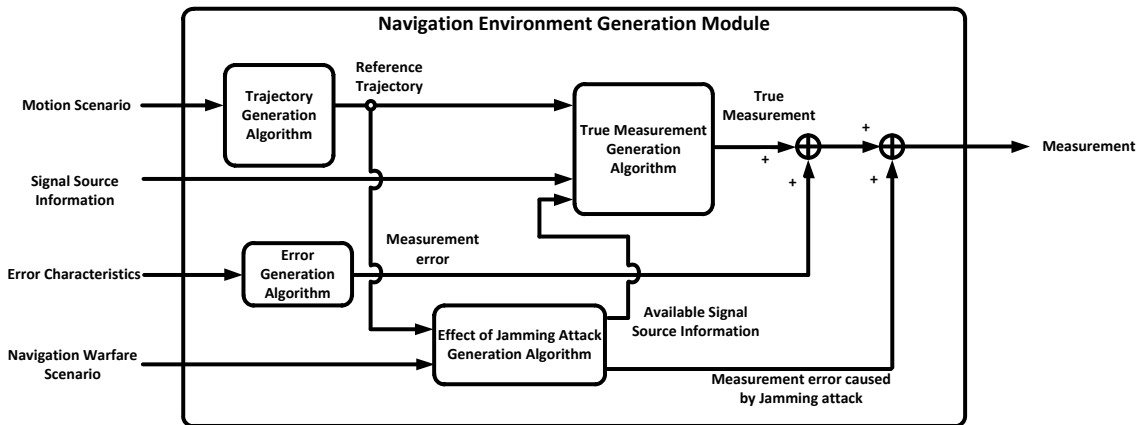


Fig. 3. Navigation environment generation module.

various parameters can be set or evaluation results are displayed through the graphical user interface (GUI).

The integrated navigation system M&S software configuration is shown in Fig. 1. The integrated navigation system M&S software consists of navigation environment generation module navigation algorithm module, analysis module, and GUI module.

Users of M&S software or developers of the navigation system can set parameters required to generate measurements by the navigation environment generation module through the GUI module. The position of the navigation signal sources based on the coverage analysis results is reflected to generate measurements in the navigation environment generation module. The navigation algorithm module performs the navigation for measurements generated by the navigation environment generation module and results are provided to users or developers through the GUI.

### 3. NAVIGATION ENVIRONMENT GENERATION MODULE

A radio navigation system consists of navigation signal

sources and receivers (Groves 2013). As shown in Fig. 2, a receiver receives signals transmitted from the navigation signal sources and generates measurements. In a navigation system using high frequency bands such as DME or VHF Omni-directional range (VOR), signals may not reach receivers as they are blocked by terrain or buildings between signal source and receiver (Groves 2013). As shown in Fig. 2, navigation environment generation means simulation of three-dimensional (3D) motion of a vehicle, characteristics of navigation signal sources, characteristics of radio propagation channels, and some parts of receivers. The errors included in the measurements can be divided into errors due to signal sources, errors occurred in the signal propagation process, and errors generated in the receiver (Kaplan & Hegarty 2006, Groves 2013). Position error, velocity error, and clock error of navigation signal sources affect measurements. Errors are generated to the characteristics of channels through which signals are transmitted. The errors generated in receivers occur when navigation signals are passed through the radio frequency front end and correlators (Kaplan & Hegarty 2006, Groves 2013). Measurements may not be obtained or large errors may occur in measurements due to jammer's attack (White et al. 1998).

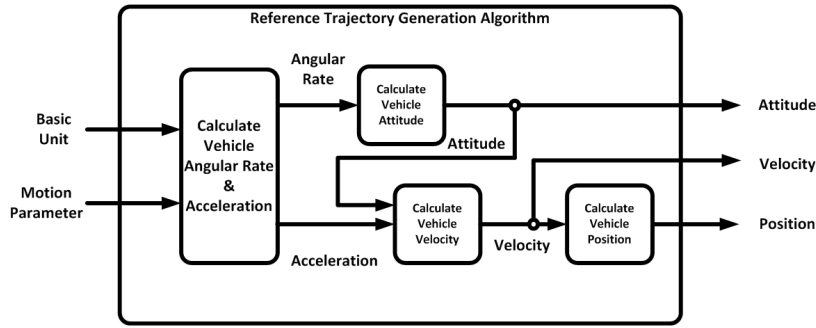


Fig. 4. Reference trajectory generation algorithm.

Considering the above characteristics, the navigation environment generation method applicable to the M&S software of the integrated navigation system is shown in Fig. 3. The navigation environment generation module consists of reference trajectory generation algorithm, signal visibility determination algorithm, true measurement generation algorithm, error generation algorithm, and jamming attack influence generation algorithm. As shown in Fig. 3, the reference trajectory is generated first from a scenario that represents the vehicle motion. Availability of signal sources is determined based on navigation warfare scenarios after determining the visibility of signal sources based on terrain information, position of navigation sources, and characteristics of navigation signals. True measurements are generated from the position of signal sources and reference trajectory. And the measurements which are inputs of the navigation algorithm are generated by adding errors occurred in signal sources, errors occurred in the navigation signal transmission process, errors occurred in the receiver, and errors occurred due to jamming attack to the true measurements.

### 3.1 Reference Trajectory Generation Algorithm

Structure of the reference trajectory generation algorithm is shown in Fig. 4. Motion of the vehicle is represented by a combination of constant acceleration, banking, rise/fall, and turning which are basic motion units. As shown in Fig. 4, angular velocity and acceleration of the vehicle are calculated from the basic motion units and related parameters. The attitude of the vehicle is calculated from the angular velocity, and vehicle's velocity is calculated from the attitude and acceleration. Finally, the position of the vehicle is calculated from the velocity.

#### 3.1.1 Calculation of angular velocity and acceleration

In case of the constant acceleration motion, acceleration is

generated as in Eq. (1) and the initial value of acceleration is zero. And angular velocity is zero.

$$a_k^{NED} [m] = a_{input}, (m \neq 1) \tag{1}$$

where  $a_k^{NED} [m]$  denotes acceleration of the  $m$ -th sample in the  $k$ -th trajectory segment, and  $a_{input}$  is the acceleration of the vehicle.

In case of the banking motion, the roll rate is the input parameter  $\dot{\phi}_{input}$ , pitch rate and yaw rate are zero. And acceleration is zero.

In case of the rise/fall motion, the pitch rate of the vehicle is the input parameter  $\dot{\theta}_{input}$ . The roll rate and yaw rate are zero. The centripetal acceleration  $|a_\theta|$  is generated from the motion parameter as in Eq. (2)

$$|a_\theta| = \frac{\|v_{init}\|^2}{\|v_{init}\|/\dot{\theta}} = \|v_{init}\|\dot{\theta} \tag{2}$$

where  $v_{init}$  denotes the initial speed of the vehicle and  $\dot{\theta}$  denotes pitch rate.

In case of the turning motion, the yaw rate is the input parameter  $\dot{\psi}_{input}$ . The roll rate and pitch rate are zero. The centripetal acceleration  $|a_c|$  is generated from the motion parameter as in Eq. (3)

$$|a_c| = |g \tan \phi_{init}| \tag{3}$$

where  $g$  denotes gravitational acceleration, and  $\phi_{init}$  the initial roll angle of the vehicle.

#### 3.1.2 Attitude calculation

In case of the constant acceleration motion, attitude is the same as the initial value.

In case of the banking motion, a roll angle is given in Eq. (4). The pitch and yaw do not change.

$$\phi_k [m] = \phi_k [m-1] + \phi_{inc}, (m \neq 1) \tag{4}$$

where  $\phi_k[m]$  denotes the roll angle of the  $m$ -th sample in the  $k$ -th trajectory segment.  $\phi_{inc}$  denotes roll angle increment per sample in Eq. (5).

$$\phi_{inc} = \frac{\phi_{target} - \phi_{init}}{\text{round}(|\phi_{target} - \phi_{init}| / \dot{\phi} \Delta t)} \quad (5)$$

where  $\phi_{target}$  denotes the target roll angle.  $\dot{\phi}$  denotes the roll rate.  $\Delta t$  is the sampling time. *round* denotes the rounding operator to the first decimal place.

In case of the rise/fall motion, the pitch angle is represented in Eq. (6). The roll and yaw do not change.

$$\theta_k[m] = \theta_k[m-1] + \theta_{inc}, \quad (m \neq 1) \quad (6)$$

where  $\theta_k[m]$  denotes the pitch angle of the  $m$ -th sample in the  $k$ -th trajectory segment.  $\theta_{inc}$  denotes the pitch angle increment per sample in Eq. (7).

$$\theta_{inc} = \frac{\theta_{target} - \theta_{init}}{\text{round}(|\theta_{target} - \theta_{init}| / \dot{\theta} \Delta t)} \quad (7)$$

where  $\theta_{target}$  denotes the target pitch angle.

In case of the turning motion, the yaw angle is given in Eq. (8). The roll and pitch do not change.

$$\psi_k[m] = \psi_k[m-1] + \psi_{inc}, \quad (m \neq 1) \quad (8)$$

where  $\psi_k[m]$  denotes the yaw angle of the  $m$ -th sample in the  $k$ -th trajectory segment.  $\psi_{inc}$  denotes the yaw angle increment per sample in Eq. (9).

$$\psi_{inc} = \frac{-\text{sign}(\psi_{init}) \psi_{amount}}{\text{round}(|\psi_{amount}| / \dot{\psi} \Delta t)} \quad (9)$$

where  $\psi_{amount}$  denotes the turning angle and *sign* denotes sign function.

### 3.1.3 Calculation of velocity

In case of the constant acceleration motion, the velocity is given in Eq. (10).

$$v_k^{ENU}[m] = v_k^{ENU}[m-1] + a_{input}(m) \Delta t, \quad (m \neq 1) \quad (10)$$

where  $v_k^{ENU}[m]$  is the velocity in the navigation coordinate system (East North Up coordinate system) of the  $m$ -th sample in the  $k$ -th trajectory segment.

In case of the banking motion, the velocity is constant as in Eq. (11).

$$v_k^{ENU}[m] = v_k^{ENU}[m-1], \quad (m \neq 1) \quad (11)$$

In case of the rise/fall motion, the velocity is given in Eq. (12).

$$v_k^{ENU}[m] = \begin{bmatrix} \cos(-\gamma) & \cos(-\gamma) & 0 \\ -\sin(-\gamma) & \cos(-\gamma) & 0 \\ 0 & 0 & 1 \end{bmatrix} \begin{bmatrix} \cos(\theta_{inc}) & 0 & -\sin(\theta_{inc}) \\ 0 & 1 & 0 \\ \sin(\theta_{inc}) & 0 & \cos(\theta_{inc}) \end{bmatrix} \begin{bmatrix} \cos(-\gamma) & \sin(-\gamma) & 0 \\ -\sin(-\gamma) & \cos(-\gamma) & 0 \\ 0 & 0 & 1 \end{bmatrix} v_k^{ENU}[m-1] \quad (12)$$

where  $\gamma$  is the direction angle in the northeast plane in Eq. (13).

$$\gamma = \tan^{-1} \left( \frac{(v_{init})_N}{(v_{init})_E} \right) \quad (13)$$

where  $(v_{init})_N$  is the velocity in the north direction at the start.  $(v_{init})_E$  denotes the velocity in the east direction at the start.

In case of the turning motion, the velocity is given in Eq. (14).

$$v_k^{ENU}[m] = \begin{bmatrix} \cos(-\psi_{inc}) & \cos(-\psi_{inc}) & 0 \\ -\sin(-\psi_{inc}) & \cos(-\psi_{inc}) & 0 \\ 0 & 0 & -1 \end{bmatrix} v_k^{ENU}[m-1], \quad (m \neq 1) \quad (14)$$

### 3.1.4 Calculation of position

The position of the vehicle is obtained from velocities of constant acceleration motion, banking motion, rise/fall motion, and turning motion.

In case of the constant acceleration motion, the position is given in Eq. (15).

$$p_k^{ENU}[m] = p_k^{ENU}[m-1] + v_{init}(m) \Delta t + 0.5 a_{input}(m) (\Delta t)^2, \quad (m \neq 1) \quad (15)$$

where  $p_k^{ENU}[m]$  is the position in the navigation coordinate system (East North Up coordinate system) of the  $m$ -th sample in the  $k$ -th trajectory segment.

In case of the banking motion, the position is given in Eq. (16).

$$p_k^{ENU}[m] = p_k^{ENU}[m-1] + v_k^{ENU}[m] \Delta t, \quad (m \neq 1) \quad (16)$$

In case of the rise/fall motion, the position is given in Eq. (17).

$$\begin{bmatrix} (p_k)_E[m] \\ (p_k)_N[m] \\ (p_k)_U[m] \end{bmatrix} = \begin{bmatrix} \gamma \cos \beta_{up/down} \cos \gamma + r \cos(\beta_{up/down} - \pi + \theta_k[m]) \cos \gamma \\ \gamma \cos \beta_{up/down} \sin \gamma + r \cos(\beta_{up/down} - \pi + \theta_k[m]) \sin \gamma \\ \gamma \sin \beta_{up/down} + r \sin(\beta_{up/down} - \pi + \theta_k[m]) \end{bmatrix} + \begin{bmatrix} (p_{init})_E \\ (p_{init})_N \\ (p_{init})_U \end{bmatrix} \quad (m \neq 1) \quad (17)$$

where  $\gamma$  is the direction angle of the vehicle in the northeast plane, and  $r$  is the rising radius of the vehicle.  $(p_{init})_E$ ,  $(p_{init})_N$  and  $(p_{init})_U$  are the components in the east, north, and up directions

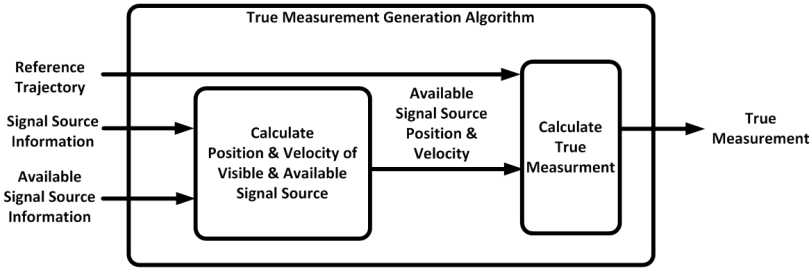


Fig. 5. True measurement generation algorithm.

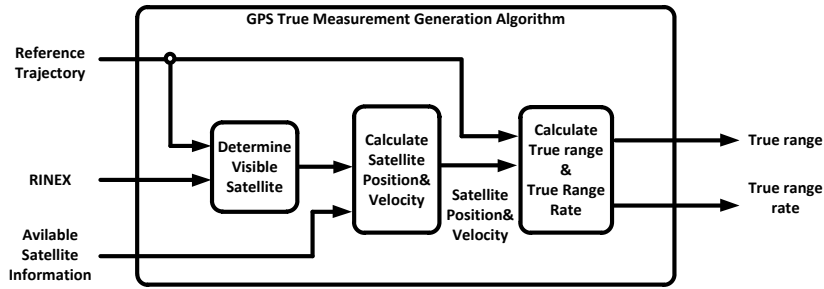


Fig. 6. GPS true measurement generation algorithm.

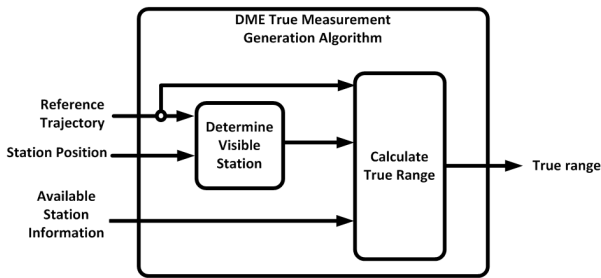


Fig. 7. DME true measurement generation algorithm.

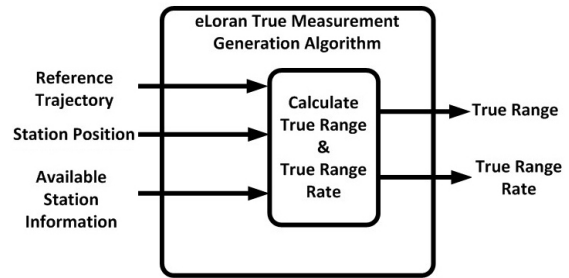


Fig. 8. eLoran true measurement generation algorithm.

of the initial position, respectively.  $(p_k)_E$ ,  $(p_k)_N$  and  $(p_k)_U$  are the position components in the east, north, and up directions at the k-th trajectory segment.  $\beta_{up/down}$  is the angle between the vector from the vehicle to the center of the rotation and the northeast plane in Eq. (18).

$$\beta_{up/down} = \tan^{-1} \frac{(v_{init})_U}{\sqrt{(v_{init})_E^2 + (v_{init})_N^2}} + \frac{\pi}{2} \text{sign}(\theta_{tangent} - \theta_{init}) \quad (18)$$

In case of the turning motion, the position is given in Eq. (19).

$$\begin{bmatrix} (p_k)_E [m] \\ (p_k)_N [m] \\ (p_k)_U [m] \end{bmatrix} = \begin{bmatrix} \gamma \cos \beta_{banking} + r \cos(\beta_{banking} - \pi + \psi_k [m]) \\ \gamma \sin \beta_{banking} + r \cos(\beta_{banking} - \pi + \psi_k [m]) \\ 0 \end{bmatrix} + \begin{bmatrix} (p_{init})_E \\ (p_{init})_N \\ (p_{init})_U \end{bmatrix} \quad (m \neq 1) \quad (19)$$

where  $\beta_{banking}$  is the angle between the vector from the vehicle

to the center of the rotation radius and the east axis in Eq. (20).

$$\beta_{banking} = \tan^{-1} \left( \frac{(v_{init})_N}{(v_{init})_E} \right) - \frac{\pi}{2} \text{sign}(\phi_{init}) \quad (20)$$

### 3.2 True measurement Generation Algorithm

The structure of the true measurement generation algorithm is shown in Fig. 5. Visibility and availability of signal sources from the navigation signal source information and available signal source information are determined first. The position and velocity of the signal sources whose visibility and availability are guaranteed are obtained, and true measurements are calculated from the position and velocity of the signal sources and reference trajectory.

Figs. 6-8 show the true measurement generation algorithm of GPS, DME, and eLoran, respectively. As shown in Fig. 6, ephemeris data are first extracted from the Receiver INdependent EXchange (RINEX) file in the true

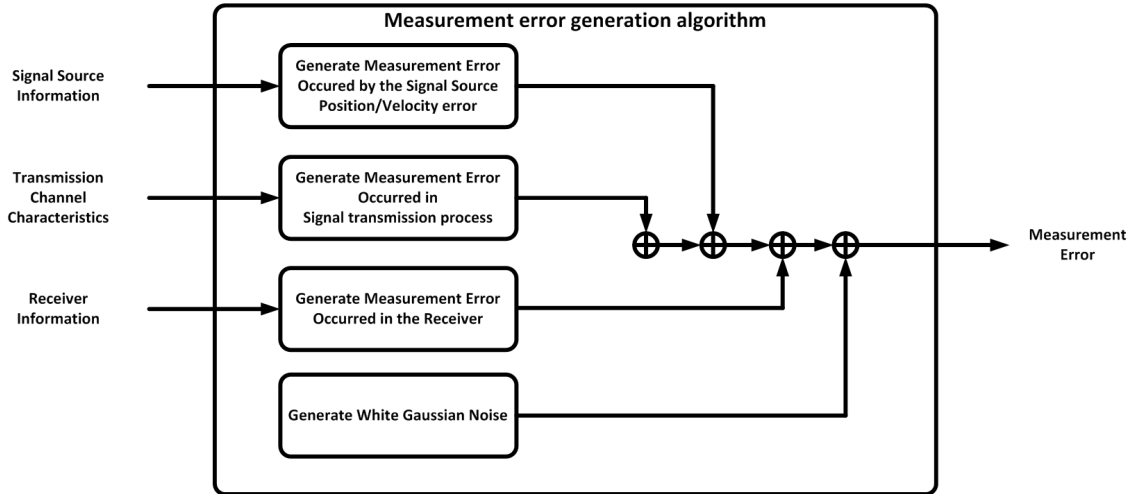


Fig. 9. Measurement error generation algorithm.

measurement generation algorithm of GPS. Visibility of satellite is determined through ephemeris data and reference trajectory. Availability of satellites is determined based on the available satellite information. After calculating the position and velocity of the satellite whose visibility and availability are guaranteed, the true range and the true range rate are generated from the position and velocity of the satellite, and reference trajectory. In the true measurement generation algorithm of DME in Fig. 7, visibility of the station is determined from the position of the DME station and reference trajectory. The true range is generated from the position of available DME station and reference trajectory. Since eLoran is rarely affected by geographic features in the signal propagation, the true range and the true range rate are generated directly from the position of available eLoran station and reference trajectory as shown in Fig. 8

### 3.3 Error Generation Algorithm

Errors due to the position and velocity uncertainty of signal sources, errors occurred in signal propagation process, errors occurred in the receiver, and white Gaussian noise are generated selectively to the characteristics of target system, operation environments of target system, and purpose. Since the integrated navigation algorithm in this paper performs navigation for measurements after correcting errors that are already known to the receiver, errors that are not compensated in the receiver are generated in the proposed navigation environment generation module and added to the true measurements. The error generation algorithm is given in Fig. 9 and Eq. (21).

$$e = e_{source} + e_{transmit} + e_{receiver} + w \quad (21)$$

where  $e_{source}$  is the position and velocity error of the signal source,  $e_{transmit}$  is the error occurred in the signal propagation process.  $e_{receiver}$  is the error occurred in the receiver, and  $w$  is a white Gaussian noise.

#### 3.3.1 Errors due to position and velocity uncertainty of signal source

In satellite navigation systems such as GPS and KPS, errors due to position and velocity uncertainty of signal source are given in Eq. (22).

$$e_{source} = \Delta D_{i,s} \quad (22)$$

where  $\Delta D_{i,s}$  is difference between satellite position calculated from ephemeris information of satellite and actual satellite position.

In terrestrial radio navigation systems, errors due to position and velocity uncertainty of signal source is given in Eq. (23).

$$e_{source} = \Delta D_{i,g} \quad (23)$$

where the position error  $\Delta D_{i,g}$  of the station is difference between station position in the receiver and actual station position.

#### 3.3.2 Errors occurred in the signal propagation process

The error in the signal propagation process of a satellite navigation system is given in Eq. (24).

$$e_{transmit} = c(\Delta T_i + \Delta I_i) \quad (24)$$

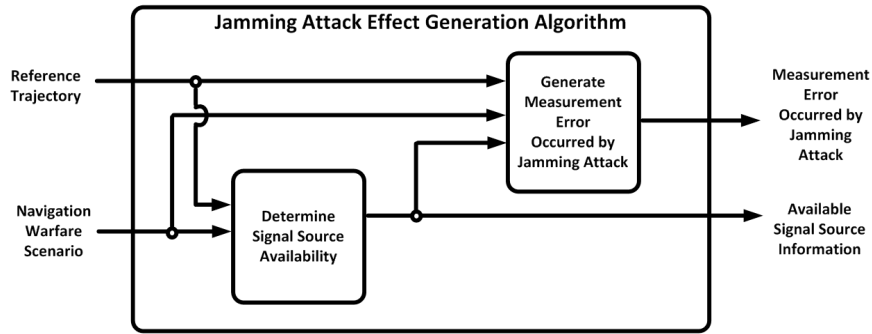


Fig. 10. Measurement error generation algorithm.

where  $c$  denotes the speed of light.  $\Delta T_i$  is the tropospheric delay error.  $\Delta I_i$  is the ionospheric delay error.

The error occurred in the signal propagation process of terrestrial radio navigation systems is given in Eq. (25).

$$e_{transmit} = \Delta\rho_{PF} + \Delta\rho_{SF} + \Delta\rho_{ASF} \quad (25)$$

where  $\Delta\rho_{PF}$  is the Primary Factor caused by difference between signal propagation speed in the atmosphere and that in free space.  $\Delta\rho_{SF}$  is the Secondary Factor which is the delay when the signal is propagated in the sea surface.  $\Delta\rho_{ASF}$  is the Additional Secondary Factor, which is the delay when the signal is propagated in the ground surface.

### 3.3.3 Errors occurred in the receiver

The error occurred in the receiver of the satellite navigation system is represented in Eq. (26).

$$e_{receiver} = c(b_{c,s} + \Delta v_s) \quad (26)$$

where  $b_{c,s}$  is the clock bias error of the receiver and  $v_s$  is thermal noise.

The error occurred in the receiver of the terrestrial radio navigation system is represented in Eq. (27).

$$e_{receiver} = c(b_{c,g} + \Delta v_g) \quad (27)$$

where  $b_{c,g}$  is the clock bias error of the receiver and  $v_g$  is the thermal noise.

### 3.4 Influence of Jamming Attack Generation Algorithm

The structure of influence of the jamming attack generation algorithm is shown in Fig. 10. The navigation warfare scenario includes jammer's position, power, frequency, and operation time length of jammer. The measurements are significantly affected as the jammer is closer to the vehicle

and jammer's power is stronger. If the influence of jamming attack is large, the algorithm determines that signal sources are not available. As shown in the figure, availability of signal source is determined first from the reference trajectory and navigation warfare scenario, and then measurement errors occurred by jamming attack for available signal sources are generated.

## 4. VERIFICATION OF THE NAVIGATION ENVIRONMENT GENERATION MODULE

To demonstrate the applicability of the proposed design method of the navigation environment generation module to an M&S software, the functions were verified first through MATLAB, and the operations of the navigation environment generation module were verified in the M&S software for integrated navigation system. Navigations were performed for the true measurements in order to verify the navigation environment generation module. The specifications of GPS and eLoran were used in the implementation. Research results of KPS were utilized for the KPS since it is at a developing stage (Choi et al. 2012, Min et al. 2017).

### 4.1 Results of Verification Through MATLAB

After the position, velocity and attitude of the vehicle were calculated for the true measurement, they were compared to the reference trajectories.

#### 4.1.1 Reference trajectory

Fig. 11 shows the reference trajectory. The vehicle is stationary for 900 sec, and in motion for 2,500 sec. The initial position of the vehicle is 35.34° of latitude, 126.19° of longitude, and 100 m of altitude. The vehicle rises up to 8 km of altitude. The vehicle moves with forming a pattern of  $\infty$  and falls.

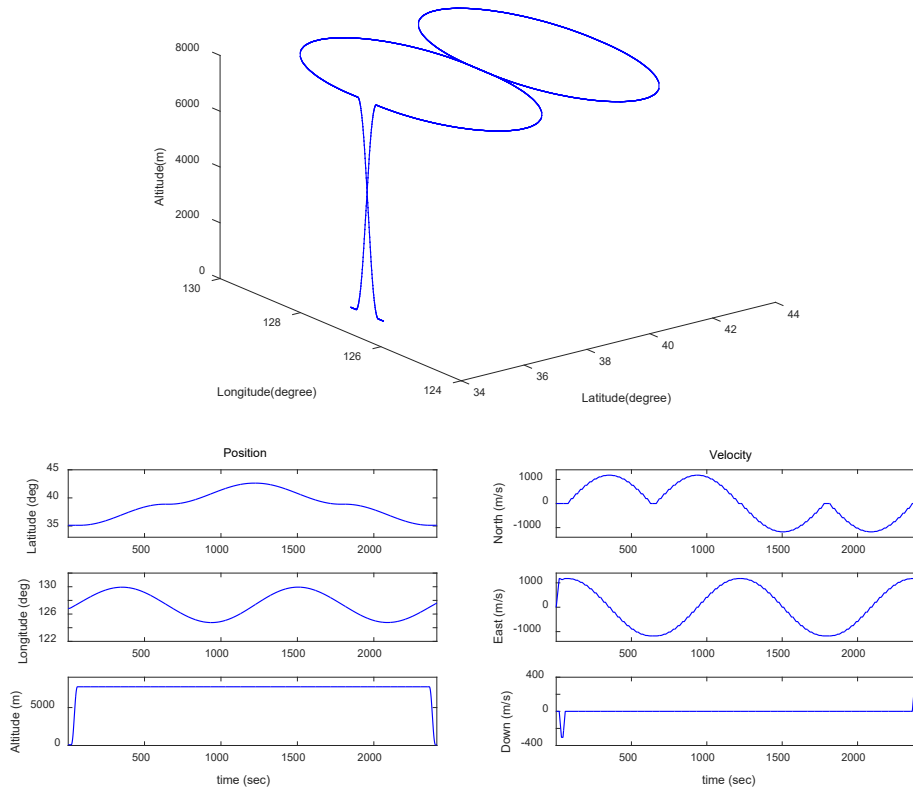


Fig. 11. Reference trajectory.

4.1.2 Results of measurement generation

Measurement generation results of GPS, KPS, and eLoran are shown in Figs. 12-14 when the vehicle is stationary for 900 sec. The figures show that the measurements change as GPS and KPS satellites move, while the measurements of eLoran are constant.

Measurement generation results of GPS, KPS, and eLoran are shown in Figs. 15-17 when the vehicle is in motion for 2,500 sec.

4.1.3 Navigation results

The navigation results of GPS, KPS, and eLoran were obtained using the least square method. The navigation results are shown in Figs. 18-20 when the vehicle is stationary for 900 sec. Navigation errors are shown in Figs. 21-23. Figures show that position errors in all navigation systems are smaller than  $10^{-8}$  m in the north, east, and down directions, and the velocity errors are also smaller than  $10^{-8}$  m/s. The Root Mean Square Error (RMSE) of the navigation results of GPS, KPS, and eLoran are presented in Table 1 when the vehicle is stationary for 900 sec. The table shows that the position errors in all navigation systems are smaller than  $5 \times 10^{-12}$  m in the north, east, and down directions, and the

Table 1. Position and velocity error when the vehicle is stationary.

	Position error (RMSE) (m)			Velocity error (RMSE) (m/s)		
	North	East	Down	North	East	Down
GPS	0	0	$3.69 \times 10^{-12}$	0	0	0
KPS	0	0	$3.69 \times 10^{-12}$	0	0	0
eLoran	0	0	0	0	0	0

Table 2. Position and velocity error when the vehicle is in motion.

	Position error (RMSE) (m)			Velocity error (RMSE) (m/s)		
	North	East	Down	North	East	Down
GPS	$2.75 \times 10^{-4}$	0	$7.04 \times 10^{-11}$	$1.66 \times 10^{-11}$	$4.56 \times 10^{-11}$	0
KPS	$2.75 \times 10^{-4}$	0	$7.04 \times 10^{-11}$	$2.48 \times 10^{-11}$	$2.48 \times 10^{-11}$	0
eLoran	$2.75 \times 10^{-4}$	0	0	$2.48 \times 10^{-11}$	$2.48 \times 10^{-11}$	0

velocity errors are zero.

Navigation results of GPS, KPS, and eLoran are shown in Figs. 24-26 when the vehicle is in motion for 2,500 sec as in Fig. 11. Navigation errors are shown in Figs. 27-29. The figures show that differences between all navigation results and the reference trajectories in Fig. 11 are less than  $6 \times 10^{-4}$  m. It can be seen that the position errors in the navigation system are smaller than  $10^{-8}$  m in the north, east, and down directions, and the velocity errors are also smaller than  $10^{-8}$  m/s. Furthermore, the RMSE of the navigation results of GPS, KPS, and eLoran are given in Table 2 when the vehicle is in motion for 2,500 sec as in Fig. 11. The table shows that the position errors in all navigation systems are smaller than  $10^{-4}$  m in the north, east,

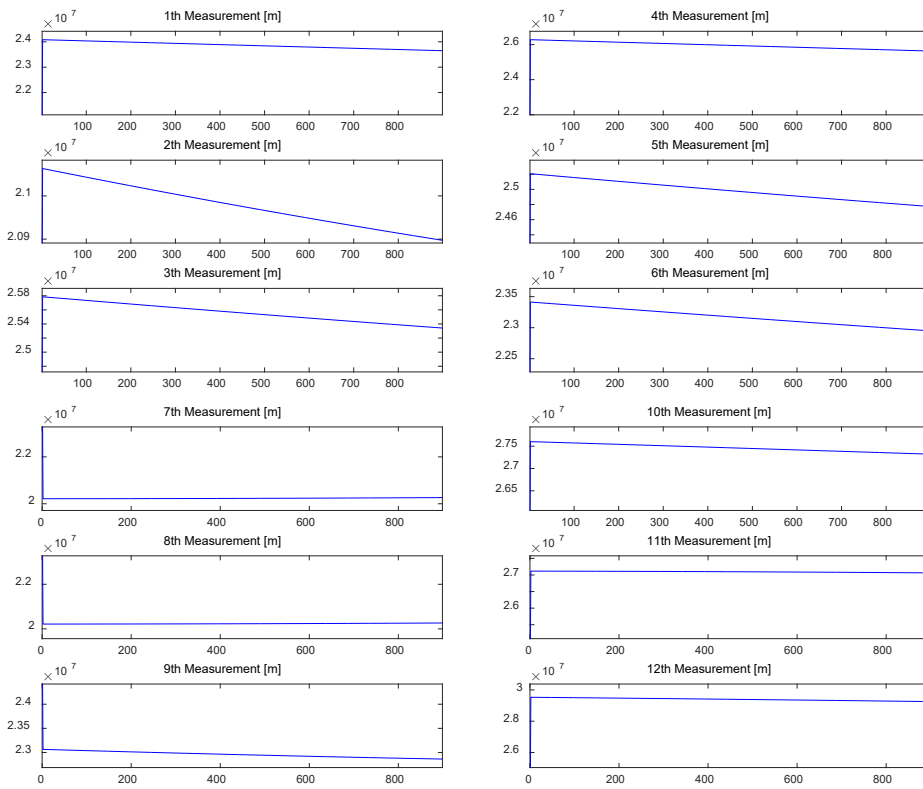


Fig. 12. GPS measurements.

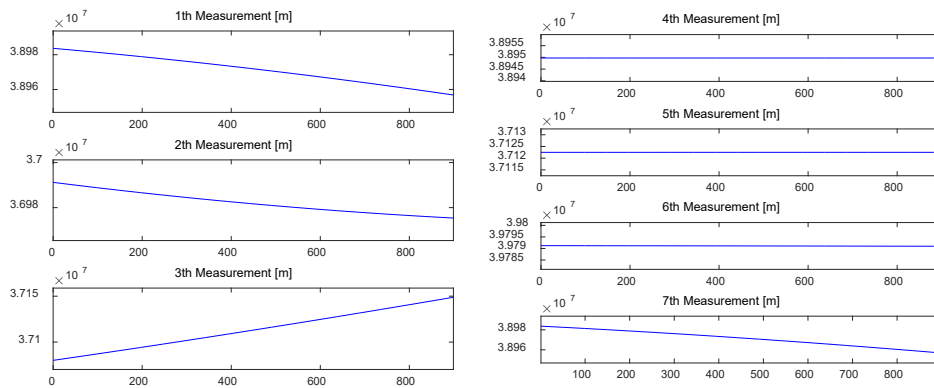


Fig. 13. KPS measurements.

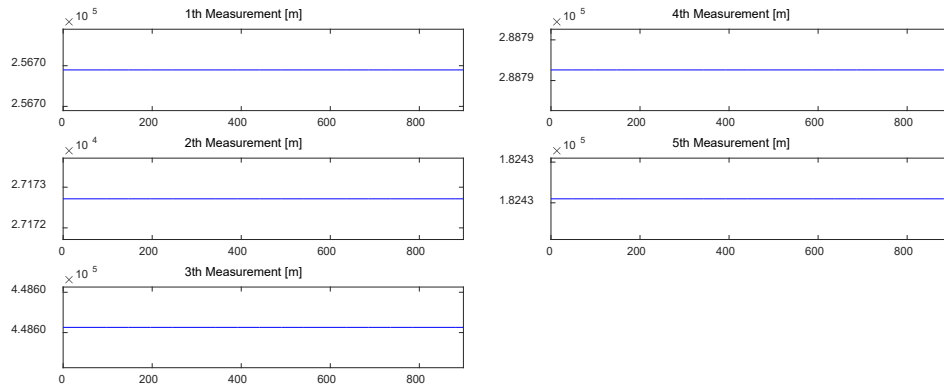


Fig. 14. eLoran measurements.

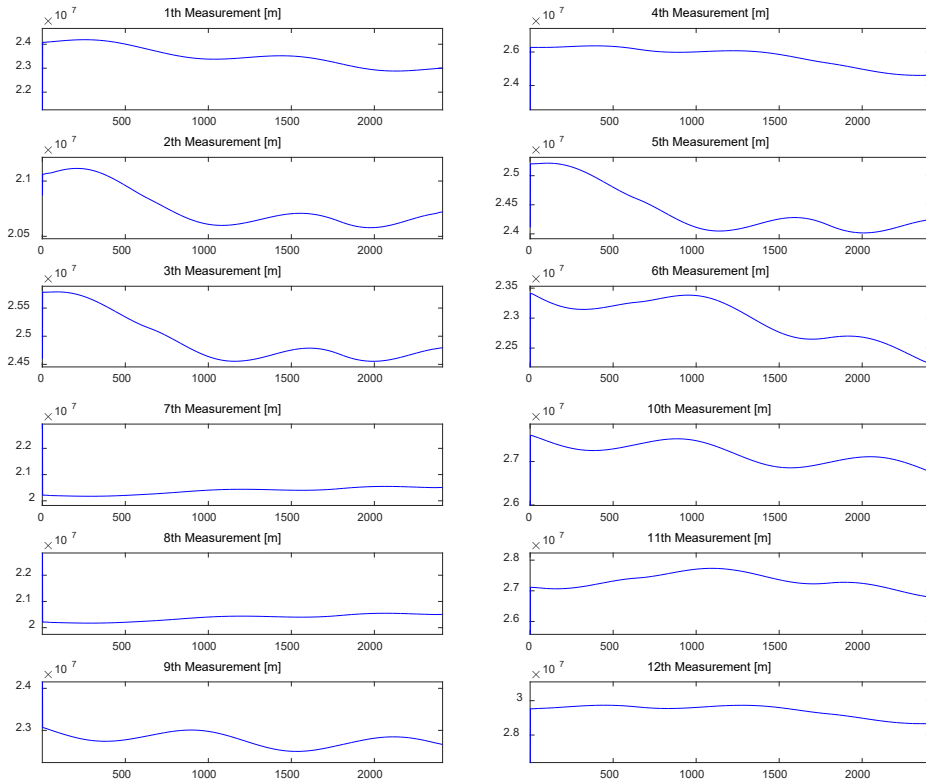


Fig. 15. GPS measurements.

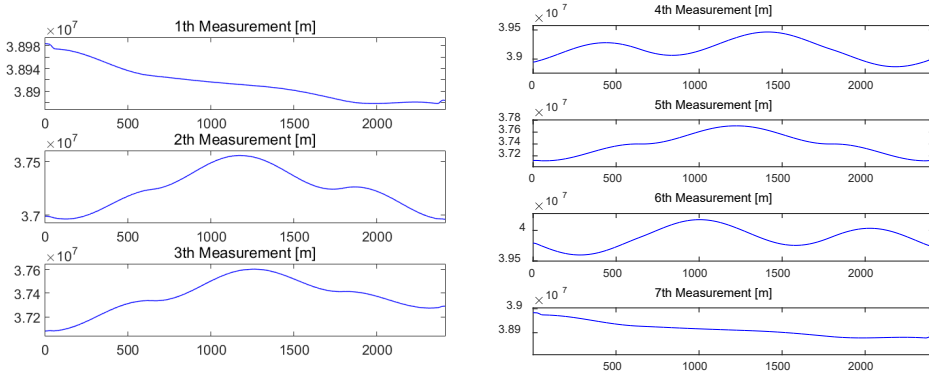


Fig. 16. KPS measurements.

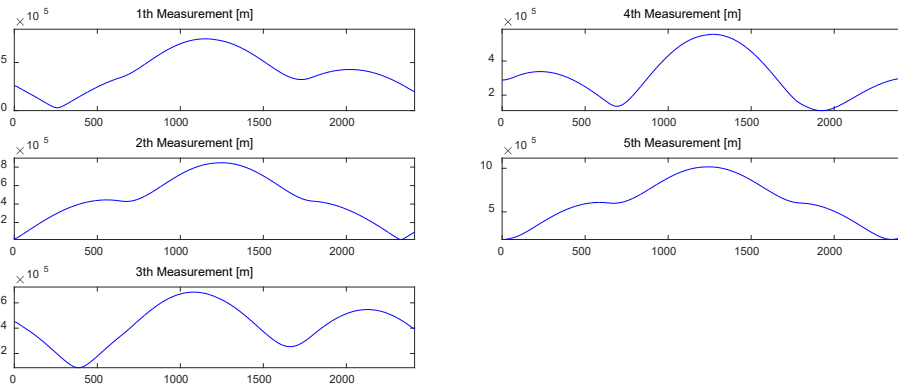


Fig. 17. eLoran measurements.

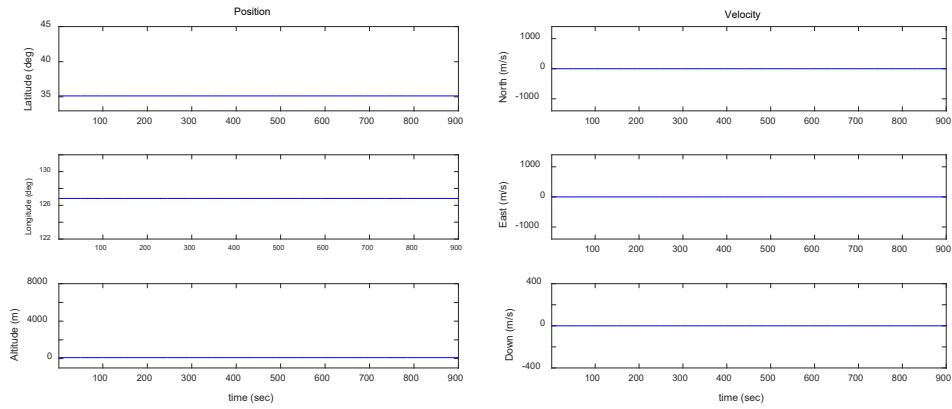


Fig. 18. GPS navigation result.

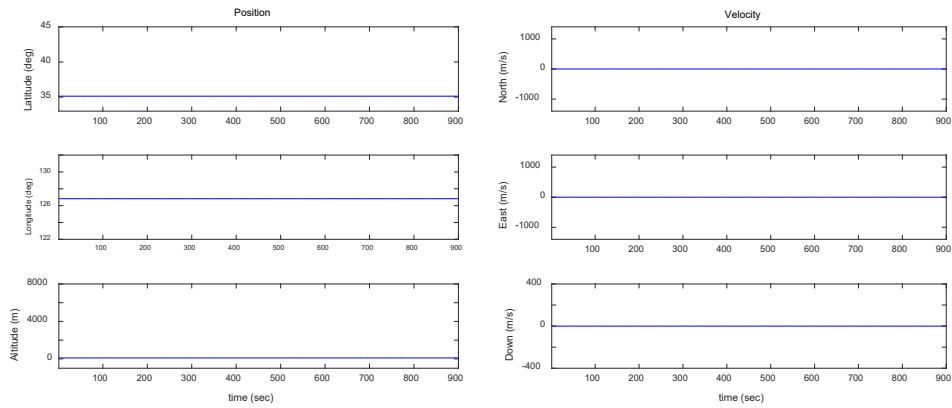


Fig. 19. KPS navigation result.

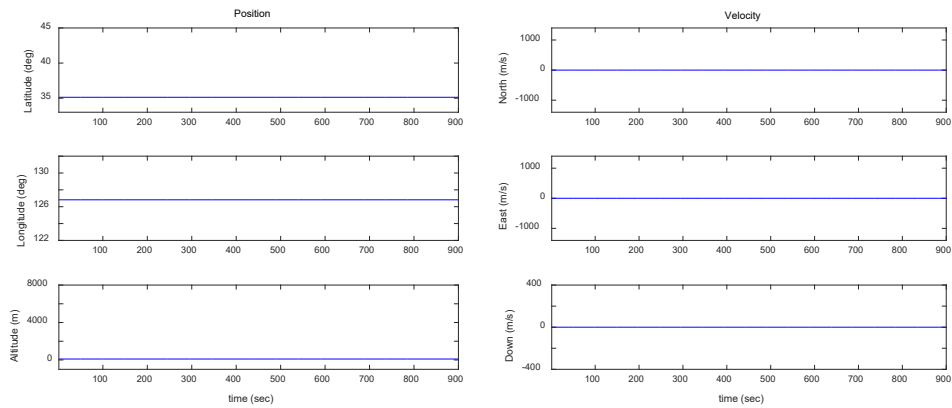


Fig. 20. eLoran navigation result.

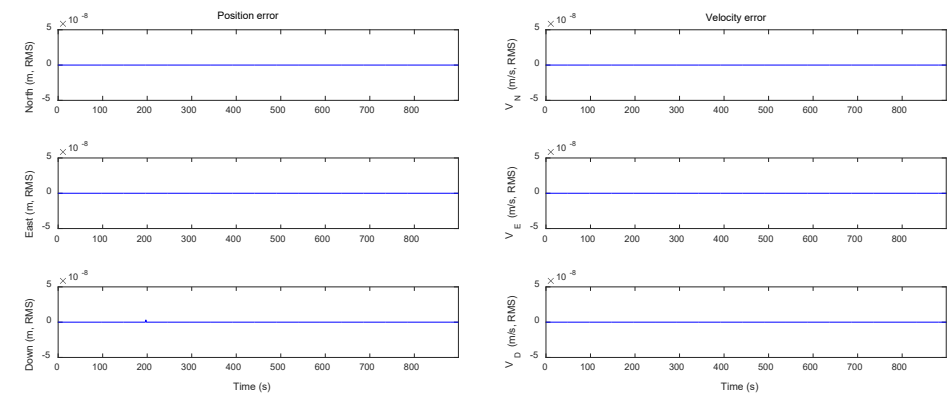


Fig. 21. GPS position error and velocity error.

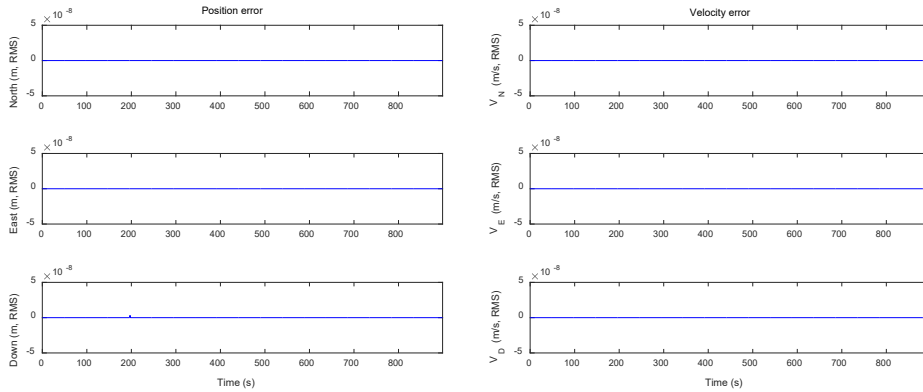


Fig. 22. KPS position error and velocity error.

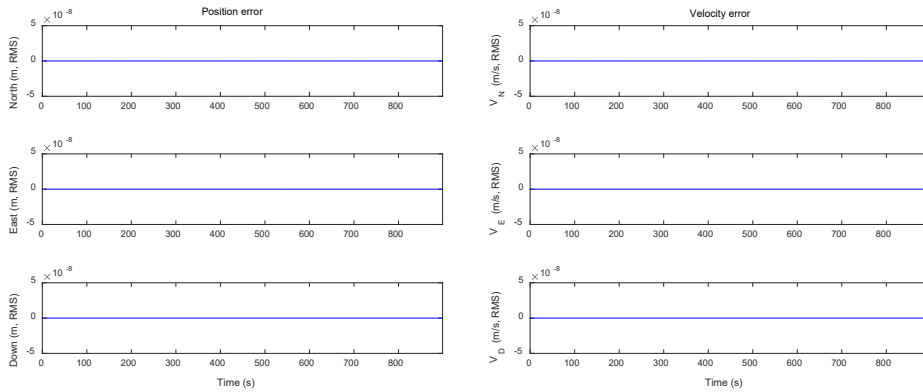


Fig. 23. eloran position error and velocity error.

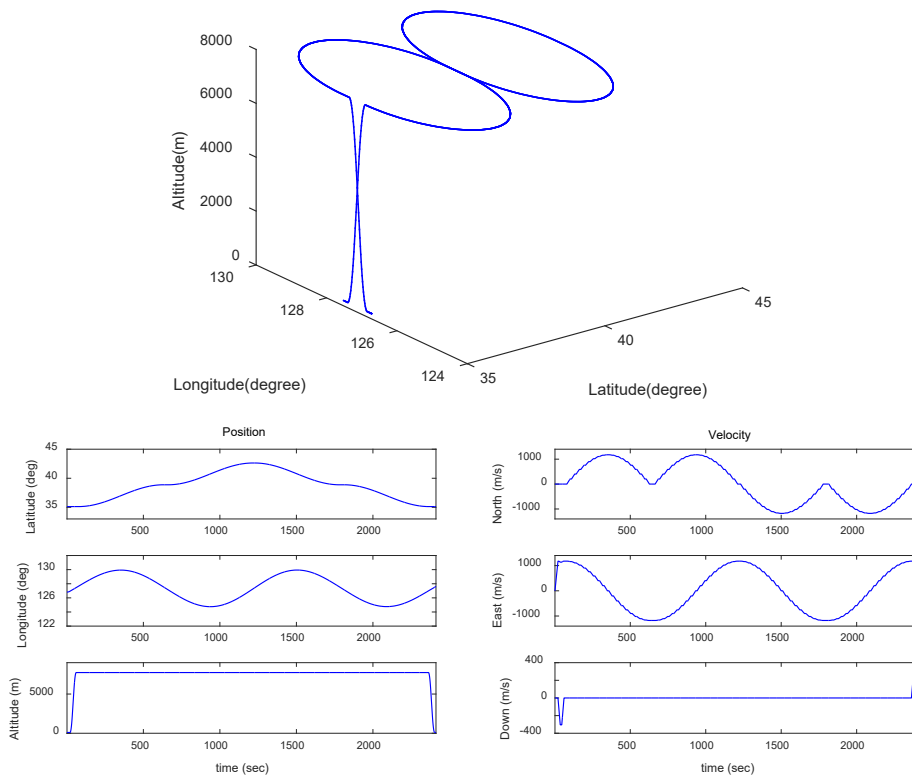


Fig. 24. GPS navigation result.

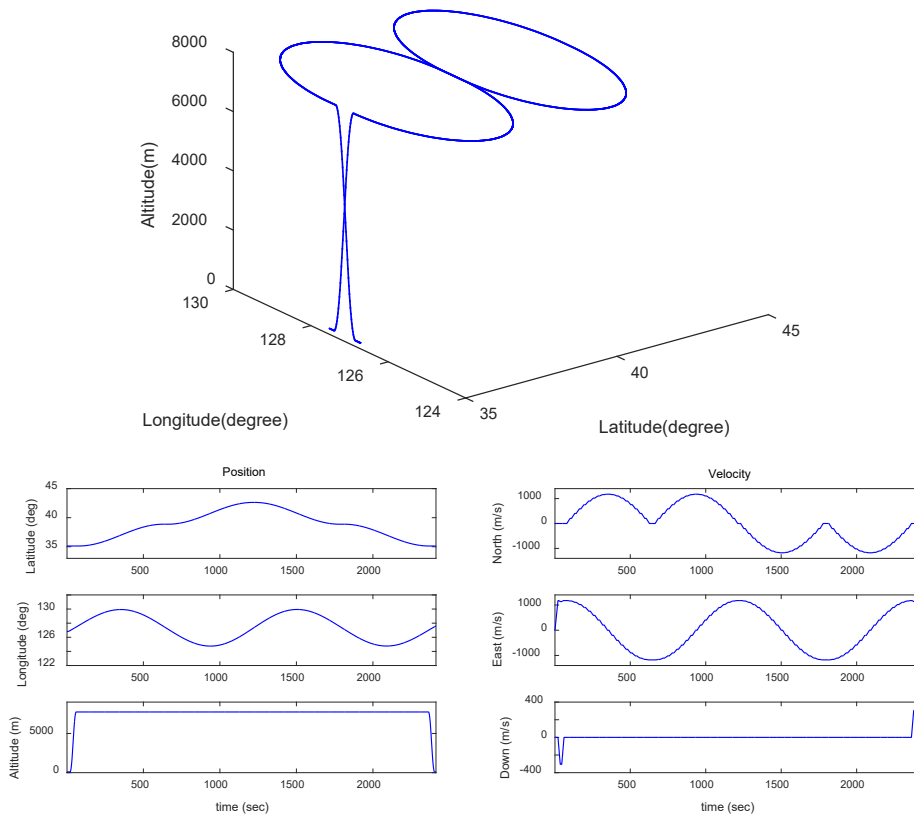


Fig. 25. KPS navigation result.

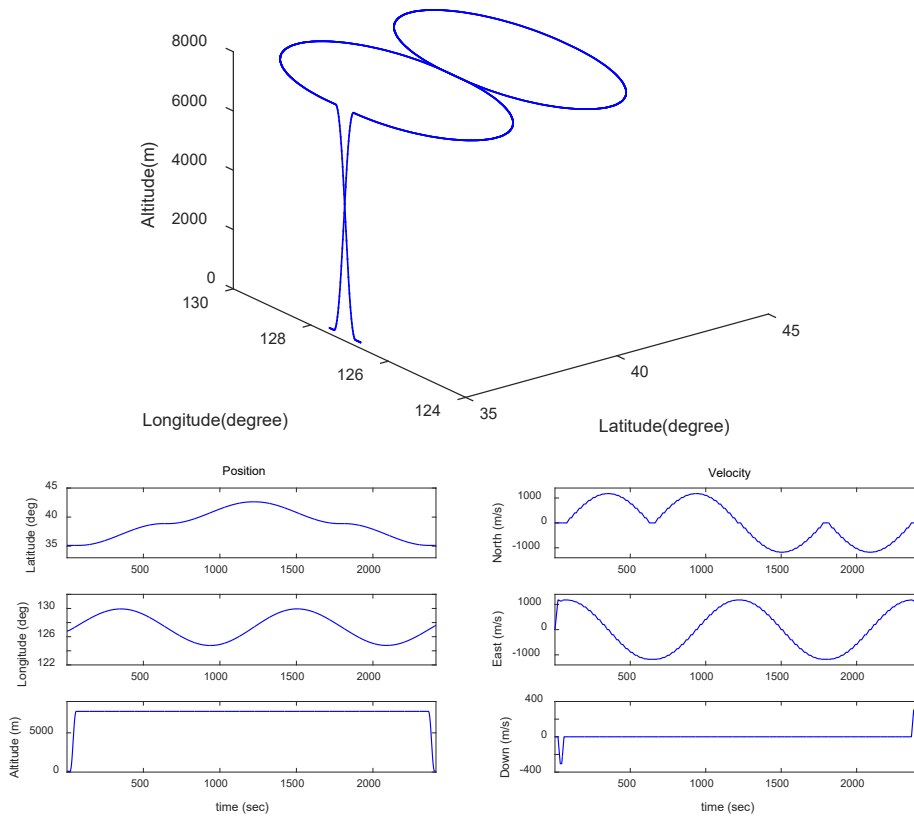


Fig. 26. eLoran navigation result.

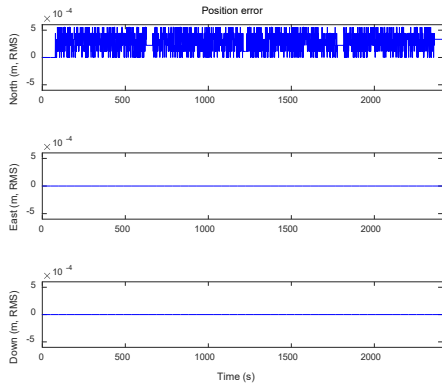


Fig. 27. GPS position error and velocity error.

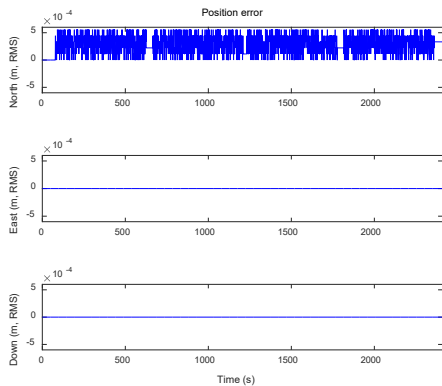
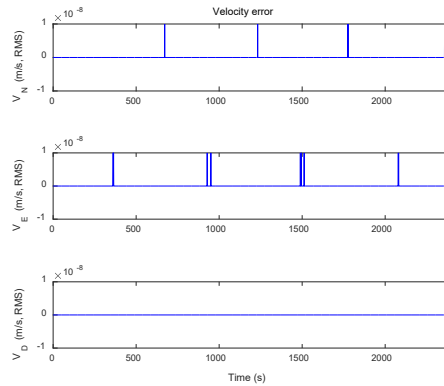


Fig. 28. KPS position error and velocity error.

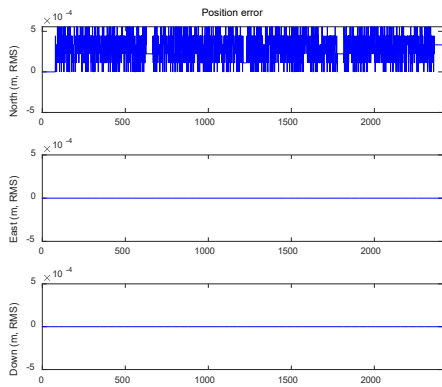
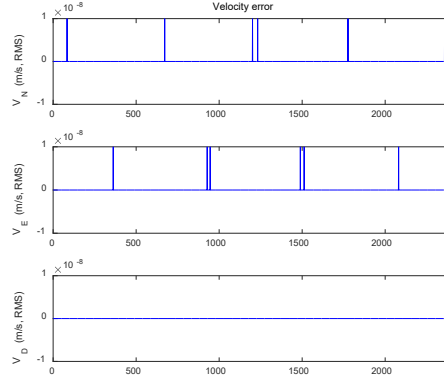
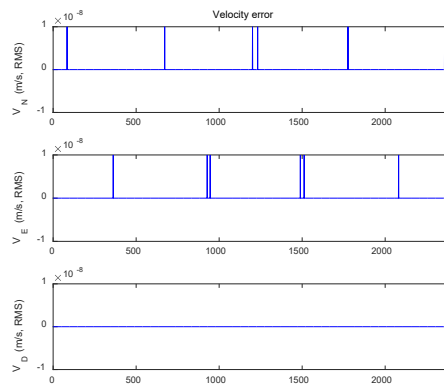


Fig. 29. eloran position and velocity error.



and down directions, and the velocity errors are smaller than  $5 \times 10^{-11}$  m/s. Errors are due to numerical errors, and the results show that the generated measurements are valid.

**4.2 Verification Through M&S Software**

To demonstrate the applicability of the proposed design method, an M&S software was implemented on Visual C++.

Parameters required to generate the navigation environment can be set through the GUI of M&S software as in Fig. 30. The initial position, velocity, attitude, and basic

motion unit of the vehicle for the generation of the reference trajectory as well as motion parameters in relation to the basic motion unit can be set as in the left window of Fig. 30. The database file of the navigation signal sources can be loaded as in the center window. The the navigation system error parameters are directly set as in the right window.

The same trajectory was generated in Fig. 11 by setting initial value, basic motion unit, and motion parameters through the GUI, and the true measurements were generated based on the same navigation signal source information as the case through MATLAB.

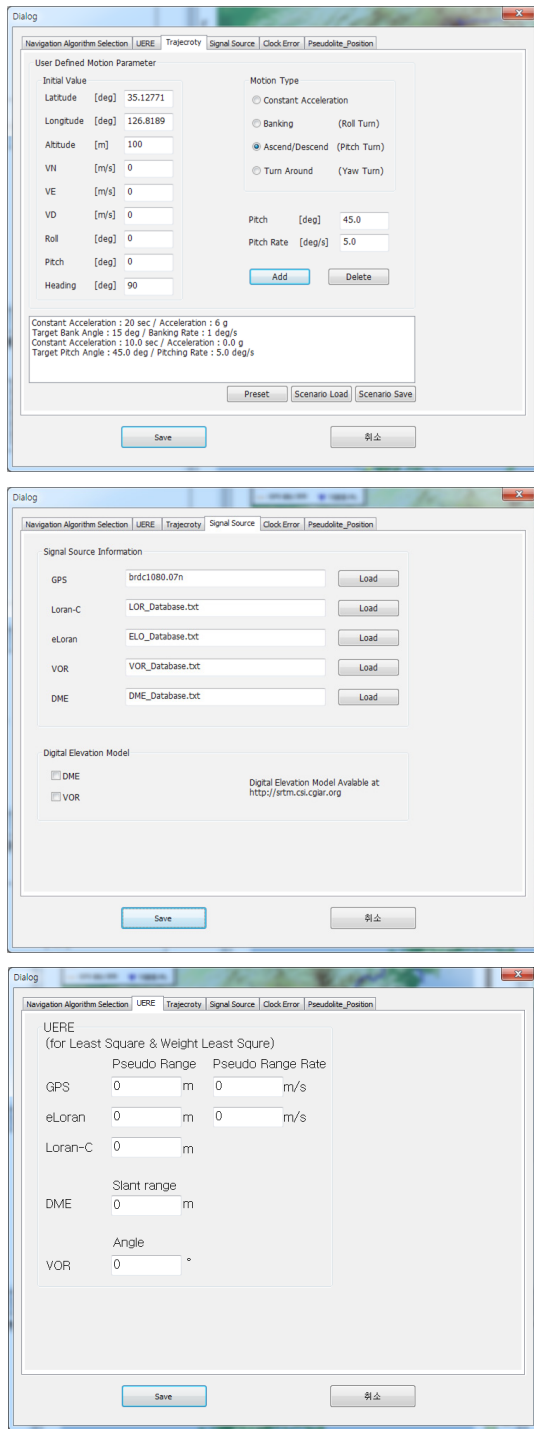


Fig. 30. Navigation environment generation parameter setting through GUI.

Result display of M&S software GUI is shown in Fig. 31. Measurements of navigation systems can be seen in the upper left window in Fig. 31, and the sky plot of GPS and KPS is in the center left window. The navigation results are shown in the lower left window, and reference trajectory, navigation results, and positions of stations of the terrestrial radio

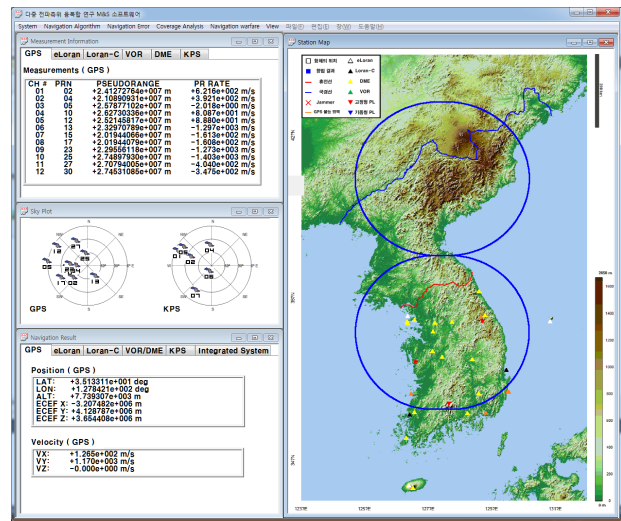


Fig. 31. Navigation result on M&S software GUI.

navigation system are shown in the right window.

## 5. CONCLUDING REMARKS AND FURTHER STUDIES

A method of designing a navigation environment generation module in M&S software of the integrated navigation system was proposed in this paper. The navigation generation module consists of reference trajectory generation algorithm, true measurement generation algorithm, and error generation algorithm. Visibility determination algorithm or jamming attack influence generation algorithm can be added to the type of navigation system, characteristics, purpose, and presence of jamming. In order to show effectiveness of the proposed navigation environment generation module design method, the functions in the module were verified first through MATLAB. And the Visual C++ based M&S software was implemented. True measurements of GPS, KPS, and eLoran were generated from the reference trajectory. Navigation results obtained from the true measurements were compared with the reference trajectories.

In the near future measurement generation algorithms of DME, VOR, Loran-c, and mobile/fixed pseudolite as well as the influence of jamming attack on measurements will be carried out.

## ACKNOWLEDGMENTS

This work has been supported by the National GNSS Research Center Program of Defense Acquisition Program

Administration and Agency for Defense Development.

## REFERENCES

- Cho, S. L., Lim, D. W., Yeo, S.-R., Park, C., Hwang, D.-H., et al. 2012, Design of Component-Based GNSS Multi-Band IF Signal Generator, Journal of the Korean GNSS Society, 1, 29-34
- Choi, M. S., Won, D. H., Jun, H. S., Kim, D. M., Sung, S. K., et al. 2012, Navigation Performance Analysis according to the Korean Navigation Satellite System Orbit Design Elements, Proceedings of the Korean Society for Aeronautical and Space Sciences, Jeju Island, Korea, 14-16 November 2012, pp.626-630
- Department of Defense. 2010, FEDERAL RADIONAVIGATION PLAN. Springfield, Virginia: National Technical Information Service.
- Department of Transportation. 2007, National PNT Architecture Workshop at Volpe, the Volpe Center.
- Dong, L., Ma, C., & Lachapelle, G. 2004, Implementation and Verification of a Software-Based IF GPS Signal Simulator, Proceedings of the 2004 National Technical Meeting of The Institute of Navigation, San Diego, California, 26-28 January 2004, pp.378-389
- Eldredge, L., Enge, P., Harrison, M., Kenagy, R., Lo, S., et al. 2010, Alternative positioning, navigation & timing (PNT) study, International Civil Aviation Organization Navigation Systems Panel (NSP) Working Group Meetings, Montreal, Canada, 11-27 May 2010, pp.1-19
- Groves, P. D. 2013, Principles of GNSS, Inertial, and Multisensor Integrated Navigation Systems, 2nd ed. (Boston: Artech House Inc.)
- Ji, H.-M., Koo, M. S., Oh, S. H., & Hwang, D.-H. 2012, GPS/IMU data Generator of the M&S Software Platform for Ultra-tightly Coupled GPS/INS Integrated Navigation System, Proc. of 2012 ICROS Conference, Seoul, Korea, 5-6 April 2012, pp.238-239
- Kaplan, E. D. & Hegarty, C. J. 2006, Understanding GPS: Principles and Applications, 2nd ed. (Boston: Artech House Inc.)
- Kim T.-H., Lee, J.-E., Lee, S.-U., Kim, J.-H., & Hwang, D.-H. 2009, Study on for Simulation of GNSS Signal Generation, Journal of the Korean Society for Aeronautical and Space Sciences, 37, 1148-1156. <https://doi.org/10.5139/JKSAS.2009.37.11.1148>
- Lee, J. H. 2007, The Theory and Practice for Modeling and Simulation as a Transformation Enabler for Efficient Defense Management, Korea Information Processing Society Review, 14, 83-95. <http://kiss.kstudy.com/thesis/thesis-view.asp?key=2649595>
- Lim, S., Shin, M. Y., Cho, S. L., Park, C., & Lee, S. J. 2008, Design of Software-based GPS Spoofing Signal Generator, Information and Control Symposium, Konkuk University, Korea, 25 April 2008, pp.63-64
- Lo, S., Enge, P., Niles, F., Loh, R., Eldredge, L., et al. 2010, Preliminary assessment of alternative navigation means for civil aviation, Proceedings of 2010 International Technical Meeting of the Institute of Navigation, San Diego, California, 25-27 January 2010, pp.314-322
- Maria, A. 1997, Introduction to modeling and simulation, Proc. of the 1997 Winter Simulation Conference, IEEE, Atlanta, Georgia, 7-10 December 1997, pp.7-13
- Min, D., Lee, J., & Lee, J. 2017, Optimal UERE Budget Allocation for KNSS Architecture Design, Proceedings of the Korean Society for Aeronautical and Space Sciences, Jeju Island, Korea, 15-18 November 2017, pp.242-243
- White, N. A., Maybeck, P. S., & DeVilbiss, S. L. 1998, Detection of interference/jamming and spoofing in a DGPS-aided inertial system, IEEE Transactions on Aerospace and Electronic Systems, 34, 1208-1217. <https://doi.org/10.1109/7.722708>
- Williams, P., Basker, S., & Ward, N. 2008, e-Navigation and the Case for eLoran, The Journal of Navigation, 61, 473-484. <https://doi.org/10.1017/S0373463308004748>



**Heyone Kim** received B.S. degree in the Department of Electronics Engineering, Chungnam National University, in 2017. His research interest includes Gyro-Free Inertial Navigation System and Modeling & Simulation Software.



**Junhak Lee** received B. S. degree and M. S. degree in the Department of Electronics Engineering, Chungnam National University in 2016, 2018, respectively. His research interest include Gyro-Free Inertial Navigation System and Kalman filtering.



**Sang Heon Oh** is a principal research engineer of the Integrated Navigation Division of Navcours Co., Ltd., Korea. He received Ph.D. degree from Chungnam National University. His research interests include GPS/INS integration system, Kalman filtering, and military application.



**Hyoungmin So** is a senior researcher of Agency for Defense Development (ADD) in Korea. He received B.S. degree in the mechanical engineering from Korea Univ. and M.S. and Ph.D. degree in the aerospace engineering from Seoul National Univ. (SNU). He worked in the field of GNSS and pseudolite receiver technology including development of SDR and vector tracking loop algorithm in SNU GNSS laboratory. Since 2011, he's been working for ADD.



**Dong-Hwan Hwang** is a professor in the Department of Electronics Engineering, Chungnam National University, Korea. He received his B.S. degree from Seoul National University, Korea in 1985. He received M.S. and Ph.D. degree from Korea Advanced Institute of Science and Technology, Korea in 1987 and 1991, respectively. His research interests include GNSS/INS integrated navigation system design and GNSS applications.